Vacancy defects in $PbTiO_3$ and lanthanide-ion-doped $PbTiO_3$: A study of positron lifetimes

R. A. Mackie,[1] A. Peláiz-Barranco,[2] and D. J. Keeble[1,*]

[1]*Carnegie Laboratory of Physics, School of Engineering, Physics, and Mathematics, University of Dundee, Dundee DD1 4HN, United Kingdom*

[2]*Facultad de Física-Instituto de Ciencia y Tecnología de Materiales, Universidad de La Habana, San Lázaro y L, Vedado, La Habana 10400, Cuba*

(Received 20 April 2010; revised manuscript received 28 June 2010; published 29 July 2010)

Positron lifetime measurements were performed on lanthanide- (Ln) ion-doped $PbTiO_3$ and identified the presence of both Pb vacancy, V_{Pb}, and Ti vacancy, V_{Ti}, related point defects. Increasing the concentration of Ln ions La to Eu resulted in an increase in the dominant contribution to the positron lifetime spectrum from V_{Pb}-related defects, consistent with donor ion substitution at the Pb site. By contrast, increasing the concentration of Dy ions decreased the ratio of V_{Pb}- to V_{Ti}-related defects. The behavior is attributed to the incorporation of Dy^{3+} ions as acceptors at Ti sites. Density-functional theory calculations of positron lifetimes for vacancy complexes, and relaxed structure monovacancy defects, in $PbTiO_3$ are reported and support the vacancy-defect assignments.

DOI: 10.1103/PhysRevB.82.024113 PACS number(s): 78.70.Bj, 77.84.Cg, 61.72.J−, 71.60.+z

I. INTRODUCTION

The ability to manipulate important material properties of the ferroelectric perovskite oxide, ABO_3, titanates, e.g., dielectric constants and piezoelectric coefficients, by impurity doping is well known.[1,2] Substitutions normally occur at either cation site; the octahedrally coordinated *B* site, or the more open 12-coordinated *A* site. Impurity ions with a valence state less than the substituted host ion are termed acceptors, those with larger valence are donor dopants. The model ferroelectric $PbTiO_3$ is commonly donor doped using the lanthanide (Ln) ion La^{3+} which substitutes for Pb^{2+}.[3] Acceptor dopants typically incorporate at the Ti site, for example, Al^{3+}, Fe^{3+}, and Cu^{2+}, all have crystal radius comparable to Ti^{4+}.[4] Pure $PbTiO_3$ cannot be prepared as a high-density bulk ceramic due to the onset of the large tetragonal distortion on cooling into the ferroelectric phase. Doping reduces this distortion and allows ceramic processing. It has been reported that lanthanide ion doping can improve the electromechanical properties of $PbTiO_3$ materials[5] and can increase the lifetime of $BaTiO_3$ multilayer ceramic capacitors.[6] Recent interest has focused on the smaller 3 +Ln ions, which may be incorporated on either cation sublattice so acting as amphoteric dopants.[6,7] Accurate x-ray diffraction measurements can provide information on the site of dopant incorporation, and the principles of defect chemistry provide a framework for predicting the consequences of impurity ion incorporation.[3,6,7] It has been proposed that the concentration of cation vacancies present during high-temperature processing may contribute toward driving Ln ion site selection.[6] Significant residual concentrations may persist to room temperature since they are assumed to act as the primary charge compensating defects.[3,7]

Early studies provided evidence that donor doping $PbTiO_3$ with La^{3+} ions resulted in charge compensation dominantly by *A*-site vacancy formation, however, it was recognized that a contribution from *B*-site vacancies was also possible.[3,8] The balance between the two mechanisms could be affected by both the lanthanum content and a quantity termed the lead elimination parameter, the number of Pb atoms eliminated per atom of La incorporated.[8] For La-doped $BaTiO_3$ the nature of the compensating cation vacancy has provided controversy, evidence that *B*-site vacancies dominant has been presented,[9] but this interpretation has been disputed.[10] The presence of cation vacancies has been inferred by fitting x-ray diffraction data using defect chemical models.[8,11] By contrast, positron annihilation spectroscopy (PAS) methods have specific sensitivity to open volume defects in materials, the positron localizes within the attractive potential well resulting from the lack of a positively charged atomic core at the vacancy defect site. PAS methods applied to Pb-based perovskite oxide materials have detected cation vacancy defects.[12–15] In particular, positron lifetime annihilation spectroscopy measurements are capable of resolving several positron states and density-functional theory (DFT) calculations of lifetime values can provide specific vacancy defect identification.[12,16] Here we present a positron lifetime study of lanthanide-ion-doped $PbTiO_3$ ceramics for the series La to Dy, and detail DFT positron lifetimes calculations for a range of vacancy defects in $PbTiO_3$.

The positron annihilates in the material from a state *i* with a lifetime τ_i and intensity I_i. This can be a delocalized state in the bulk lattice or a localized state at a vacancy defect. If vacancy defects are present the average lifetime, $\bar{\tau}=\Sigma_i I_i \tau_i$, is greater than the bulk lattice lifetime, τ_B, a characteristic quantity of the material under study. The rate of positron trapping to a vacancy defect, κ_d, is proportional to the defect concentration, $[d]$, and the constant of proportionality is the defect-specific trapping coefficient, μ_d; $\kappa_d=\mu d[d]$. The one-defect simple trapping model (STM) predicts two experimental positron lifetime components, the second has a fixed value characteristic of the positron trapping defect, $\tau_2=\tau_d$, and the first has a value reduced below the bulk lifetime, $\tau_1<\tau_B$, by an amount that depends on the rate of trapping to the defect, κ_d,[17] which is given by the expression,

$$\kappa_d = \mu_d[d] = I_2\left(\frac{1}{\tau_1} - \frac{1}{\tau_2}\right). \quad (1)$$

The model is readily extended to more than one defect; this results in the appropriate number of fixed lifetime components, with values characteristic of the defects, and a reduced bulk component with a lifetime and intensity that reduces with increasing defect trapping.[17] Saturation trapping onsets when the concentration of vacancy defects increases to the point where the large majority of positrons annihilate from the defects; the reduced bulk lifetime intensity becomes negligible, and its lifetime value too short to detect. It is relevant for this work to consider the consequences of saturation trapping into two defects, in this limit the two defect STM predicts a lifetime spectrum with two components with lifetime values, τ_1 and τ_2, characteristic of the two defect types. The ratio of the two component intensities is given by the ratio of the products of the specific trapping coefficient and the defect concentration,

$$\frac{I_2}{I_1} = \frac{\kappa_{d2}}{\kappa_{d1}} = \frac{\mu_{d2}[d_2]}{\mu_{d1}[d_1]} \quad (2)$$

and hence provide a measure of relative concentration.

Ion size is an important factor in determining the site of occupation of an impurity ion used to dope a perovskite oxide. Table I gives available Shannon crystal radii for relevant ions,[4] 6 and 12 coordination correspond to the *B* and *A* site, respectively, and are directly applicable, cubic coordination is also included due to the limited number of 12 coordination values. A study of the smaller Ln ions, Dy, Ho, and Er, in Mn-codoped $PbTiO_3$ inferred from trends in the tetragonality, and enthalpy change at the Curie temperature, that the ions were incorporating mainly at the *B* site.[18] Similar studies have been performed on Ln-doped $Pb(Zr_xTi_{1-x})O_3$ (PZT) samples where measurements of weight loss were used to infer the percentage occupancy on the two sites for the ions La, Nd, Eu, Gd, and Er. The results suggested that *A*-site occupancy falls from 100% for La to ~20% for Er.[19] A comparison of La and Dy doping of thin film PZT showed a variation in lattice parameter with composition suggesting that Dy incorporated at the *B* site and Raman measurements supported the assignment.[20]

II. POSITRON LIFETIME CALCULATIONS

Positron lifetime calculations were performed using DFT method implemented in the MIKA/DOPPLER package,[21] where the electron density of the solid is approximated by the nonself-consistent superposition of free atom electron densities in the absence of the positron (the so-called "conventional scheme").[22] This approximation to the complete two-component DFT (TCDFT) has been found to give positron lifetimes close to TCDFT as well as experimental values. In our calculations of the positron lifetimes used the electron-positron enhancement factor due to Barbiellini *et al.*,[23,24] as a parametrization of the data of Arponen and Pajanne,[25] (referred to as AP), described within the generalized gradient approximation of the enhancement factor. The AP enhancement has been found to give positron lifetime values in good agreement with experiment for perovskite oxides.[12,26] Recently first-principles calculations have been reported for atomic relaxations in the local structure of monovacancy defects in $PbTiO_3$;[27,28] DFT calculations using ultrasoft pseudopotentials report relaxations for the O, Ti, and Pb monovacancies in the tetragonal phase,[27] and hybrid DFT—Hartree-Fock (HF) was used to calculate the relaxed structure of the oxygen vacancy in the cubic phase.[28] Positron lifetime calculations were performed for unrelaxed and relaxed structure monovacancy defects in $PbTiO_3$, using 1080 atom $6\times6\times6$ supercells. Both the room-temperature *P*4*mm* structure,[29,30] and the high-temperature *Pm*3*m* cubic phase,[30] were used. In addition, a series of calculations were performed for range of unrelaxed cation vacancy complex and cluster defects in tetragonal $PbTiO_3$,[29] using similar supercells.

TABLE I. Shannon crystal radius values (pm) for relevant ions in 6, 8, and 12 coordination (Ref. 4).

	6	8	12
Pb^{2+}	133	143	163
Nd^{2+}		143	
Sm^{2+}		141	
Eu^{2+}	131	139	
Dy^{2+}	121	133	
La^{3+}	117.2	130	150
Nd^{3+}	112.3	124.9	141
Sm^{3+}	109.8	121.9	138
Eu^{3+}	108.7	120.6	
Gd^{3+}	107.8	119.3	
Dy^{3+}	105.2	116.7	
Ti^{4+}	74.5	88	

III. EXPERIMENT

The lanthanide-ion-doped $PbTiO_3$ ceramics were prepared by a conventional solid-state process from oxide precursors and characterized by powder x-ray diffraction,[31] 2.0 and 8.0 at. % La-, Nd-, Sm-, Eu-, Gd-, and Dy-doped samples were studied. The sample densities were greater than 88%, the average was 94%. The positron lifetime experiments were performed using a conventional fast-fast spectrometer in colinear geometry with a time resolution function of 210 ps. All spectra contained at least 5×10^6 counts. Positron sources were made from aqueous NaCl containing ^{22}Na and were deposited on thin support and protective foils, both 1 μm Ni and 8 μm Kapton, with strengths in the range ~200–500 kBq. Two near identical samples sandwiched the positron source between them. The lifetime spectrum analyzed as a sum of exponential decay components, $n(t) = \Sigma_i I_i \exp(-t/\tau_i)$, convoluted with three Gaussians describing the timing resolution function of the spectrometer. Decay components due to annihilations in the positron source were subtracted in the procedure, one component with a lifetime of ~430 ps described annihilations in the $^{22}NaCl$ crystal-

TABLE II. Positron lifetime values (ps) calculated by the DFT method MIKA for monovacancy defects in $PbTiO_3$, the relaxed local structures are given in parentheses. Tetragonal phase local relaxations were obtained from Ref. 27 and the cubic phase relaxation from Ref. 28.

Crystal structure ref.	T (K)	Bulk	V_O	V_{OI}	V_{OII}	V_{Ti}	V_{Pb}
29	295	161		167 (181)	164 (171)	203 (185)	292 (290)
30	300	162		168	165		
30	800	153	159 (156)				

lites, and had an intensity that depended on source strength, the foil component had a lifetime of ~380 ps for Kapton (~10%) or 140 ps for Ni (~10%). Care is required to correctly account for source annihilations, measurements were made with both Kapton and Ni foil sources to establish source independent fittings.[32] The fit chi-squared values for the positron lifetime results shown were all less than 1.05.

IV. RESULTS AND DISCUSSION

A. Positron lifetimes in $PbTiO_3$

The DFT calculated positron lifetimes for unrelaxed and relaxed monovacancy defects in $PbTiO_3$, obtained using MIKA/DOPPLER with AP enhancement, are shown in Table II. The bulk lifetime and the unrelaxed monovacancy lifetime values are in satisfactory agreement with those reported previously,[12,16] though are slightly larger. Applying the first-principles calculated local relaxation to the Ti vacancy resulted in a significant reduction in the lifetime from 203 to 185 ps.[27] A similar reduction, from 195 to 184 ps, was obtained previously for the relaxation of the Ti vacancy in $SrTiO_3$, and found to be consistent with the lifetime value of ~181 ps inferred from experiment.[26]

Previous positron lifetime measurements on dense ceramic PZT samples with $x=0.42$, both undoped (UD) and Fe ion doped, exhibited saturation trapping with a first lifetime component value, for UD and low Fe-doped samples, of 182(4) ps attributed to *B*-site vacancies.[12] It should also be noted that earlier calculations of the unrelaxed V_B lifetime showed an increase from 191 ps at $x=0$ to 204 ps for $x=0.4$, however, the agreement between the experimental *B*-site vacancy lifetime and the DFT value for the relaxed structure remains satisfactory.

The calculated positron lifetime for the Pb vacancy reduces very slightly, from 292 to 290 ps, on applying the first-principles calculated local relaxation,[27] again this is in agreement with results obtained for the relaxation of the *A*-site vacancy in $SrTiO_3$.[26] Positron lifetime measurements on crystal $PbTiO_3$ reported a defect lifetime component at ~280 ps, attributed to Pb vacancies.[12]

The unrelaxed oxygen vacancy positron lifetime in $PbTiO_3$ shows the smallest increase above the bulk value of 161 ps. For the room-temperature tetragonal structure, the calculated apical OI oxygen ion vacancy lifetime of 167 ps is slightly larger than the in-plane OII ion value, 164 ps (Table II). The ultrasoft pseudopotential DFT calculated relaxations were performed using the tetragonal structure,[27] when these are applied and the oxygen vacancy positron lifetime calculated, a ~10 ps increase in the lifetime value results (Table II). The hybrid DFT-HF calculations used the high-temperature cubic phase structure,[28] hence positron lifetime calculations were also performed using the 300 and 800 K structures reported by Kuroiwa *et al.*[30] The bulk structure positron lifetime increased to 153 ps at 800 K and the unrelaxed oxygen vacancy lifetime to 159 ps. The markedly different DFT-HF local relaxation resulted in a *reduction* in this lifetime by 3 ps to 156 ps.

While the agreement between relaxed structure cation vacancy theoretical positron lifetime values and the experimental values for perovskite oxide titanates is good, larger experimental values have been observed from some samples. Previous measurements on Fe-doped PZT reported second lifetime values varying from 280 to 293 ps,[12] and a similar study of Nb- and La-doped PZT reported values in the range ~290–305 ps.[13] The limited experimental resolution means that when there is a positron trapping vacancy-related defect with a lifetime τ_i additional vacancy defects with lifetimes in the approximate range $\tau_i < \tau < 1.4 \times \tau_i$ will not be resolved, and a single, weighted average, lifetime component is detected. The observation of experimental lifetime components larger than the monovacancy values suggest larger vacancy complex defects can also be present. Table III shows the calculated positron lifetime values for a series of unrelaxed vacancy complex and cluster defects in $PbTiO_3$.

From Table III it can be seen that removing the short bond apical OI oxygen ion nearest neighbor at the Ti site increased the lifetime from 203 to 221 ps, also removing the long bond OI ion further increased the defect value to 258 ps. Removing one of the next-nearest-neighbor apical Ti ions from this complex increased the lifetime to 270 ps. Removing nearest-neighbor oxygen ions at the 12-coordinated Pb vacancy site

TABLE III. Positron lifetime values (ps) calculated by the DFT method MIKA for vacancy complexes in $PbTiO_3$, obtained using the room-temperature structure given in Ref. 29.

$V_{Ti\text{-}OI}$	$V_{Ti\text{-}2OI}$	$V_{2Ti\text{-}2OI}$	$V_{Pb\text{-}O}$	$V_{Pb\text{-}4O}$	$V_{2Pb\text{-}2O}$	$V_{2Pb\text{-}3O}$	$V_{Ti\text{-}3O\text{-}Pb}$	$V_{Ti\text{-}3O\text{-}2Pb}$
221	258	270	296	306	310	317	344	371

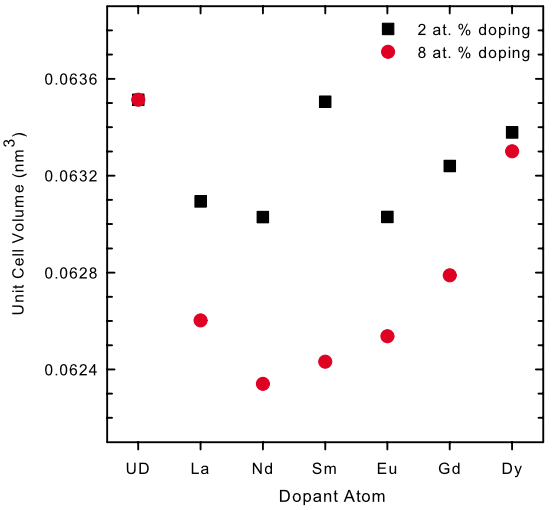

FIG. 1. (Color online) Unit-cell volume against Ln ion obtained from lattice parameters measured by x-ray diffraction. It should be noted that weak x-ray peaks attributed to a secondary phase of $SmTi_2O_7$ were observed for the 2 at. % Sm-doped sample.

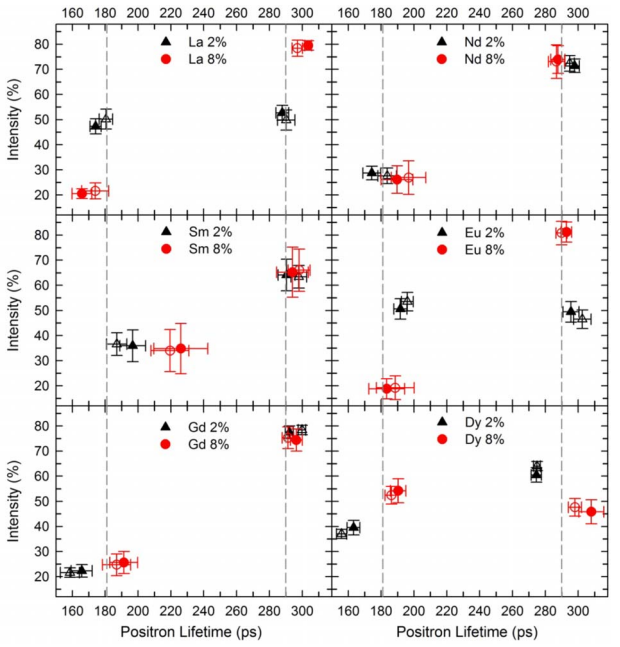

FIG. 2. (Color online) Positron lifetime measurements for the series of Ln-ion-doped ceramic $PbTiO_3$ samples, both 2 at. % (triangle-up) and 8 at. % doped (circle) samples shown. Measurements made using both a Kapton foil supported positron source (closed symbols) and a Ni foil supported source (open symbols). The lifetime values 181 and 290 ps are shown using dashed lines.

had a less marked effect; adding one oxygen vacancy increased the lifetime from 292 to 296 ps, removing a further three oxygen ions increased this to 306 ps. Removing two Pb ions and two adjacent oxygen ions increased the lifetime to 310 ps, and adding a third oxygen vacancy increased the defect complex lifetime to 317 ps.

Creating a vacancy cluster by removing both a Pb and a Ti cation, with three oxygen nearest neighbors, increased the lifetime significantly to 344 ps. Removing an additional neighbor Pb increased this further to 371 ps (Table III). These vacancy complex and cluster results are consistent with similar calculations for $SrTiO_3$.[33] Previous DFT positron lifetime calculations for V_A-V_O and V_B-V_O defects in $SrTiO_3$ have performed using both Boronski and Nieminen (BN),[26,34] and AP,[26] enhancement, show good agreement for the increase in lifetime resulting from complex formation. However, it has been shown that the AP values are in closer agreement with experiment for the perovskite oxide titanates.[12,26] The AP calculations were extended to cation vacancy-multi V_O complexes,[26] and to complexes with involving several cation vacancies (Table III).[33] Positron lifetime measurements in thin film $SrTiO_3$ have observed defects with a lifetime of ~400 ps, providing evidence for the possible formation of large vacancy cluster defects in perovskite oxide titanates.[33]

B. Lanthanide-ion-doped $PbTiO_3$

Detailed structural and differential scanning calorimetry characterizations of the samples studied here have been reported in Ref. 31. The introduction of La was found to result in a marked reduction in the *c*-axis lattice constant, compared to UD $PbTiO_3$, and the magnitude of the reduction increased with increasing dopant concentration. This is consistent with the substitution of donor La^{3+} ions at the Pb site. However, further decreasing the Ln ion size resulted in a gradual recovery of the *c* parameter toward the UD value. The variation in the *a* parameter was less marked and the resulting behavior of the cell volume is shown in Fig. 1. This recovery toward the UD sample values with decreasing Ln ion size is attributed to the onset of partial substitution of Ln ions at the *B* site.

The positron annihilation lifetime spectra from all the samples studied were found to give the lowest variance fits for two lifetime components, and the results for doping with the Ln ions La to Dy, at both 2 and 8 at. % concentrations, are shown in Fig. 2 and Table IV. The average lifetime values were all be greater than ~230 ps, significantly larger than the $PbTiO_3$ bulk positron lifetime of ~160 ps (Table II). Further, no lifetime component with a value less than τ_B was detected. It was concluded that saturation positron trapping to vacancy defects occurred in all the samples studied. The $[d]$ at which saturation trapping onsets depends on the values of τ_B and μ_d. Assuming a plausible specific trapping coefficient $\sim 2\times 10^{15}$ s^{-1} at. for a negatively charged monovacancy,[17] it can be estimated ($\kappa_d\tau_B=\mu_d[d]\tau_B\approx 10$) that saturation should occur when the vacancy concentrations exceeds ~50 ppm. There are currently no direct measurements of defect specific trapping coefficients for vacancies in oxides, however, theoretical estimates for the coefficients have been made and found to be on the order of the values inferred for vacancy defects in semiconductors and metals.[17]

The second lifetime component value was found to be in the range ~287–303 ps, except for Dy (275 ps), while the first lifetime was observed to be either ~160 ps or in the range ~175–200 ps, with the expectation of the 8 at. % Sm-doped sample which gave a value ~220 ps (Fig. 2 and Table IV). Comparing these values to the DFT-calculated

TABLE IV. Experimental positron lifetimes (ps) for Ln-ion-doped $PbTiO_3$. The values are the average of those obtained using the different positron sources after source correction.

Ln ion	Sample (at. %)	τ_1	I_1	τ_2	$\bar{\tau}$
La	2	177(4)	49(4)	289(5)	235
	8	170(7)	21(3)	300(3)	273
Nd	2	179(6)	28(3)	296(3)	263
	8	193(10)	27(6)	287(5)	262
Sm	2	192(7)	36(5)	294(5)	257
	8	223(14)	34(9)	296(8)	271
Eu	2	194(4)	52(4)	299(5)	244
	8	186(11)	19(4)	291(3)	271
Gd	2	162(6)	22(2)	296(2)	267
	8	189(9)	25(4)	294(4)	268
Dy	2	160(4)	38(2)	275(4)	231
	8	188(4)	53(4)	303(6)	242

positron lifetimes shown in Table II it is concluded that the observed first lifetime components with lifetime values in the range $\tau_1 \sim 175-220$ ps are dominated by positron trapping to Ti vacancy-related defects. Similarly, the second lifetime components, $\tau_2 \sim 275-303$ ps, are attributed to dominant positron trapping to Pb vacancy-related defects.

It can be inferred from the positron lifetime values shown in Table II that in samples exhibiting saturation trapping to defects the observation of a lifetime component value less than ~175 ps can be attributed to oxygen vacancy defects, either monovacancies or vacancy complexes, e.g., divacancies.[12] Previous variable energy PAS measurements on PZT thin films have observed sensitivity to oxygen deficiency.[14,35]

The observed second component lifetime value for the Ln ions studied had an average value of 293(7) ps (Fig. 2 and Table IV), the intensity of this component was greater than 65% for all the 8 at. % doped samples, except Dy. The component intensity increased slightly, or markedly, with increasing Ln ion concentration for the ions La to Eu. The average lifetime of this Pb vacancy-related defect component, suggests V_{Pb}-nV_O defect complexes make a contribution.

In $PbTiO_3$ large Ln ions (Table I) are expected to substitute for Pb, predominantly as donor ions in the 3+ charge state. The resulting charge can be compensated either by the generation of electronic carriers in the conduction band or by the formation of negatively charged cation vacancy defects or through a combination of both. The results presented here show cation vacancy defects are present at concentrations greater than the threshold for saturation positron trapping (~50 ppm) in all the samples studied. The results also demonstrate that for the ions La to Gd, at high dopant concentrations, the dominant cation vacancies are V_{Pb}-related defects. However, it should be noted that results also show that a significant minority concentration of V_{Ti}-related defects is also normally present.

In the saturation positron trapping regime, assuming two positron trapping defects, the simple trapping model predicts two experimental lifetime components with lifetime values characteristic of the two defects, and with intensities given by Eq. (2); the ratio defect-specific trapping coefficients is a constant for a given pair of defect types. Accurate values for $\mu_{V_{Ti}}$ and $\mu_{V_{Pb}}$ are not known, however there is evidence that $\mu_{V_{Ti}} \geq \mu_{V_{Pb}}$.[12] Variations in the intensities of two saturation trapped defect lifetime components with a material parameter such as dopant concentration can provide a direct measure of changes in the relative concentration of the two dominant vacancy defects, assuming the type the vacancy defects present remains constant.

The behavior of the second experimental positron lifetime component, with increasing dopant concentration, was found to be similar for La and Eu, and for Nd, Sm, and Gd (Fig. 2 and Table IV). The La- and Eu-doped samples exhibit a marked increase in the intensity of the second lifetime component, at ~295 ps from ~50% to ~80%, with a concomitant decrease in first lifetime component (~174 ps and ~190 ps, respectively) intensity, when the dopant concentration is increased from 2 to 8 at. %. In the case of Eu a large increase in V_{Pb} defects on increasing the doping level could result if both Eu^{3+} and Eu^{2+} ion substitution at the *A* site occurred at low concentrations (Table I) but the later was suppressed at higher concentrations. For La, however, the 3+ charge state is known to be highly stable.

The Nd-, Sm-, and Gd-doped samples show a high intensity, ~65–78 %, in the second lifetime component at ~295 ps at 2 at. % doping, but on increasing to 8 at. % neither the lifetime value or intensity changed markedly. Changes were observed in the value of the first lifetime. The estimated defect concentration threshold for the onset of saturation positron trapping is of the order 100 times smaller than the charge compensation vacancy-defect concentration expected from 2 at. % 3+ ion donor doping. If Pb vacancy formation was the predominant charge compensation mechanism, ~100% intensity in a single V_{Pb}-related component would already be observed for 2 at. % doping.

By contrast, the behavior of the second lifetime component for the Dy-doped samples was markedly different, the lifetime value increases from ~275 to ~303 ps with increased doping and the intensity *decreases* from ~62% to

~47%. On closer inspection it was observed that the intensity value for the second lifetime component in the Gd-doped samples showed a small decrease, from ~78% to ~75%, with increases dopant concentration; all the larger Ln ions show either a small, or a marked, increase with increasing concentration (as discussed above).

The first component lifetime also exhibited similarities for the two smaller ions, Gd and Dy, values of ~162 ps and ~160 ps, respectively, were observed for the 2 at. % doped samples. These are significantly below the V_{Ti} value and can be attributed to significant positron trapping to oxygen monovacancies or larger oxygen vacancy complex defects, see Table II and Ref. 12. Increasing the doping to 8 at. % increased the lifetime values to ~189 ps and 188 ps, respectively (Table IV), due to a dominant contribution to the first component from V_{Ti}-related defects.

Two previous positron lifetime studies have been performed on acceptor-ion-doped PZT, both used Fe, which incorporates predominately in the 3+ charge state at the *B* site.[12,36] Both provide evidence, a significant contribution to positron trapping at vacancy-related defects with a lifetime less than the V_{Pb} lifetime, measurements on PZT ceramics where the Fe concentration was varied from 0.1 to 1.0 at. % showed a systematic relative increase in trapping to *B*-site vacancy-related defects, at the expense of trapping to Pb vacancy-related defects.[12] These results are consistent with a systematic decrease in the concentration of V_{Pb} defects with increasing Fe, or an increase in V_B defects, or a combination of both trends [Eq. (2)]. The defect concentration threshold for the onset of saturation positron trapping is at least ten times below the minimum acceptor ion concentration used. Substitution of Fe^{3+} ions at the *B* site requires compensation of excess negative charge, hence a suppression of cation vacancies could be expected with increasing $[Fe^{3+}]$. A possible explanation for the observed positron lifetime results for Fe-doped PZT would be a preferential suppression of grown-in Pb vacancies, resulting PbO loss, with respect to a constant, or more slowly reducing, residual concentration *B*-site vacancies. However, it is not clear which mechanisms could cause such a preferential suppression.

The behavior observed for Dy doping in this study is in good agreement with that previously observed for Fe acceptor ion doping in PZT. The decrease in the relative concentration of V_{Pb}- to V_{Ti},-related defects with increasing Dy concentration is a reversal of the trend observed for the larger Ln ions, Eu to La. It is inferred that these results provide evidence for the existence of a fraction of Dy ions substituting at the Ti site in the +3 charge state, acting as acceptor ions. This is supported by the behavior of the unit-cell volume with Ln ion type and concentration shown in Fig. 1. The variation in the intensity of the V_{Pb}-related positron component suggests the reversal of behavior onsets at Gd.

V. CONCLUSIONS

Atomic superposition density-functional theory calculations of positron lifetime values for unrelaxed monovacancy defects in $PbTiO_3$ were found to be in satisfactory agreement with earlier studies.[12,16] Relaxing the local structure of the cation vacancies was found to significantly reduce the lifetime for the Ti vacancy from 203 to 185 ps while the Pb vacancy value remained approximately constant at ~290 ps. Similar changes in the lifetime values had been previously observed for the Ti and Sr vacancies in $SrTiO_3$ on applying local structure relaxation.[26] Two different local relaxation structures have been reported for the oxygen vacancy in $PbTiO_3$,[27,28] the ultrasoft pseudopotential DFT-calculated relaxation increases the positron lifetime while the hybrid DFT-HF relaxation predicts a lifetime value smaller than the unrelaxed structure calculation value. Positron lifetime values were also calculated for a range of cation vacancy complex and cluster defects in $PbTiO_3$.

Positron lifetime measurements on lanthanide-ion-doped $PbTiO_3$ ceramics for the series La to Dy, using two doping concentrations, 2 and 8 at. %, show saturation positron trapping to vacancy-related defects for all samples. Trapping to Pb vacancy-related defects normally dominated. However, significant trapping to Ti vacancy-related defects was also observed. The behavior of the intensity of positron trapping to Pb vacancy-related defects with increasing Ln ion concentration was observed to reverse for Dy, compared to the ions Eu to La. The Dy ion positron trapping behavior was analogous to that observed previously for Fe acceptor ion doping in $Pb(Zr_{0.42},Ti_{0.58})O_3$. It was concluded that partial substitution of Dy^{3+} ions at the Ti site was occurring. This was consistent that the behavior of the lattice parameters which showed a recovery toward the undoped $PbTiO_3$ values with decrease in Ln ion size. The positron lifetime results also suggest partial occupancy of the Ti site occurs for Gd. The results for the large Ln ions, La to Eu, are consistent with substitution at the Pb site as donors resulting in excess charge compensation by cation vacancy defect formation.

ACKNOWLEDGMENTS

A.P.-B. and D.J.K. thank the Royal Society of London for short-term visitor and international travel awards. R.A.M. acknowledges the support from the Carnegie Trust for the Universities of Scotland. A.P.-B. also thanks the Third World Academy of Sciences (RG/PHYS/LA Grants No. 99-050, No. 02-225, and No. 05-043), and the ICTP, Trieste-Italy, for financial support for the Latin-American Network of Ferroelectric Materials (NET-43), and to R. de Lahaye Torres.

*d.j.keeble@dundee.ac.uk

[1] S. Aggarwal and R. Ramesh, Annu. Rev. Mater. Sci. **28**, 463 (1998).
[2] D. Damjanovic, Rep. Prog. Phys. **61**, 1267 (1998).
[3] D. Hennings and K. H. Härdtl, Phys. Status Solidi A **3**, 465 (1970).
[4] R. D. Shannon, Acta Crystallogr., Sect. A: Cryst. Phys., Diffr., Theor. Gen. Crystallogr. **32**, 751 (1976).
[5] T. Suwannasiri and A. Safari, J. Am. Ceram. Soc. **76**, 3155 (1993).
[6] Y. Tsur, A. Hitomi, I. Scrymgeour, and C. A. Randall, Jpn. J. Appl. Phys. **40**, 255 (2001).
[7] D. M. Smyth, *The Defect Chemistry of Metal Oxides* (Oxford University Press, New York, 2000).
[8] D. Hennings and G. Rosenstein, Mater. Res. Bull. **7**, 1505 (1972).
[9] F. D. Morrison, A. M. Coats, D. C. Sinclair, and A. R. West, J. Electroceram. **6**, 219 (2001).
[10] D. M. Smyth, J. Electroceram. **9**, 179 (2002).
[11] P. P. Neves, A. C. Doriguetto, V. R. Mastelaro, L. P. Lopes, Y. P. Mascarenhas, A. Michalowicz, and J. A. Eiras, J. Phys. Chem. B **108**, 14840 (2004).
[12] D. J. Keeble, S. Singh, R. A. Mackie, M. Morozov, S. McGuire, and D. Damjanovic, Phys. Rev. B **76**, 144109 (2007).
[13] S. Gottschalk, H. Hahn, A. G. Balogh, W. Puff, H. Kungl, and M. J. Hoffmann, J. Appl. Phys. **96**, 7464 (2004).
[14] D. J. Keeble, B. Nielsen, A. Krishnan, K. G. Lynn, S. Madhukar, R. Ramesh, and C. F. Young, Appl. Phys. Lett. **73**, 318 (1998).
[15] Y.-J. He and L.-T. Li, Acta Phys. Sin. **32**, 697 (1983).
[16] V. J. Ghosh, B. Nielsen, and T. Friessnegg, Phys. Rev. B **61**, 207 (2000).
[17] R. Krause-Rehberg and H. S. Leipner, *Positron Annihilation in Semiconductors* (Springer-Verlag, Berlin, 1999).
[18] O. P. Martinez, J. M. Saniger, E. T. Garcia, J. O. Flores, F. C. Pinar, J. C. Llopiz, and A. P. Barranco, J. Mater. Sci. Lett. **16**, 1161 (1997).
[19] A. Garg and T. C. Goel, J. Mater. Sci.: Mater. Electron. **11**, 225 (2000).
[20] H. Nakaki, H. Uchida, K. Nishida, M. Osada, H. Funakubo, T. Katoda, and S. Koda, Jpn. J. Appl. Phys. **44**, 6905 (2005).
[21] T. Torsti, T. Eirola, J. Enkovaara, T. Hakala, P. Havu, V. Havu, T. Höynälänmaa, J. Ignatius, M. Lyly, I. Makkonen, T. T. Rantala, J. Ruokolainen, K. Ruotsalainen, E. Räsänen, H. Saarikoski, and M. J. Puska, Phys. Status Solidi B **243**, 1016 (2006).
[22] M. J. Puska and R. M. Nieminen, Rev. Mod. Phys. **66**, 841 (1994).
[23] B. Barbiellini, M. J. Puska, T. Korhonen, A. Harju, T. Torsti, and R. M. Nieminen, Phys. Rev. B **53**, 16201 (1996).
[24] B. Barbiellini, M. J. Puska, T. Torsti, and R. M. Nieminen, Phys. Rev. B **51**, 7341 (1995).
[25] J. Arponen and E. Pajanne, Ann. Phys. (N.Y.) **121**, 343 (1979).
[26] R. A. Mackie, S. Singh, J. Laverock, S. B. Dugdale, and D. J. Keeble, Phys. Rev. B **79**, 014102 (2009).
[27] F. F. Ge, W. D. Wu, X. M. Wang, H. P. Wang, Y. Dai, H. B. Wang, and J. Shen, Physica B **404**, 3814 (2009).
[28] Y. F. Zhukovskii, E. A. Kotomin, S. Piskunov, and D. E. Ellis, Solid State Commun. **149**, 1359 (2009).
[29] R. J. Nelmes and W. F. Kuhs, Solid State Commun. **54**, 721 (1985).
[30] Y. Kuroiwa, S. Aoyagi, A. Sawada, J. Harada, E. Nishibori, M. Takata, and M. Sakata, Phys. Rev. Lett. **87**, 217601 (2001).
[31] A. Peláiz-Barranco, Y. Méndez-González, D. C. Arnold, D. J. Keeble, and P. Saint-Grégoire, arXiv:1007.3720 (unpublished).
[32] S. McGuire and D. J. Keeble, J. Appl. Phys. **100**, 103504 (2006).
[33] D. J. Keeble, R. A. Mackie, W. Egger, B. Löwe, P. Pikart, C. Hugenschmidt, and T. J. Jackson, Phys. Rev. B **81**, 064102 (2010).
[34] A. S. Hamid, A. Uedono, T. Chikyow, K. Uwe, K. Mochizuki, and S. Kawaminami, Phys. Status Solidi A **203**, 300 (2006).
[35] T. Friessnegg, S. Aggarwal, R. Ramesh, B. Nielsen, E. H. Poindexter, and D. J. Keeble, Appl. Phys. Lett. **77**, 127 (2000).
[36] W. Puff, N. Balke, H. Kungl, M. J. Hoffmann, and A. G. Balogh, Phys. Status Solidi C **4**, 3839 (2007).